Vibrational Strong Coupling Hot Paper

How to cite: *Angew. Chem. Int. Ed.* **2020**, *59*, 10436–10440
International Edition: doi.org/10.1002/anie.202002527
German Edition: doi.org/10.1002/ange.202002527

On the Role of Symmetry in Vibrational Strong Coupling: The Case of Charge-Transfer Complexation

Yantao Pang, Anoop Thomas, Kalaivanan Nagarajan, Robrecht M. A. Vergauwe, Kripa Joseph, Bianca Patrahau, Kuidong Wang, Cyriaque Genet, and Thomas W. Ebbesen**

Abstract: *It is well known that symmetry plays a key role in chemical reactivity. Here we explore its role in vibrational strong coupling (VSC) for a charge-transfer (CT) complexation reaction. By studying the trimethylated-benzene–I_2 CT complex, we find that VSC induces large changes in the equilibrium constant K_{DA} of the CT complex, reflecting modifications in the $\Delta G°$ value of the reaction. Furthermore, by tuning the microfluidic cavity modes to the different IR vibrations of the trimethylated benzene, $\Delta G°$ either increases or decreases depending only on the symmetry of the normal mode that is coupled. This result reveals the critical role of symmetry in VSC and, in turn, provides an explanation for why the magnitude of chemical changes induced by VSC are much greater than the Rabi splitting, that is, the energy perturbation caused by VSC. These findings further confirm that VSC is powerful and versatile tool for the molecular sciences.*

Molecular vibrations play a critical role in various chemical processes such as reactions, electron transfer, and charge transport, and much effort has been directed towards analyzing their effects, in particular by laser excitation of selected modes to influence the outcome.[1–7] Nevertheless, such a technique is often limited by intramolecular vibrational-energy redistribution (IVR) in the sample, requiring cryogenic temperatures. An alternative approach is to use vibrational strong coupling (VSC), whereby a vibrational transition of a molecule is hybridized with the zero-point energy fluctuations of a cavity mode, that is, in the absence of any light source. This has been shown to strongly impact chemical reactivity[8–13] and has the advantage that it occurs in the dark and, therefore, is not affected by IVR. VSC results in the formation of two so-called vibropolaritonic states, P+ and P–, separated in energy by the Rabi splitting $\hbar\Omega_R$ as illustrated in Figure 1 a.[14] Depending on the reaction under consideration, reactivity has been found to either slow down or be catalyzed by VSC.[8–13] Furthermore, it is possible to tilt the reactivity landscape to favor one product over another.[11] Temperature studies revealed that the thermodynamics of activation, that is, $\Delta H^{\neq}$ and $\Delta S^{\neq}$, are strongly modified by VSC, sometimes even changing sign, reflecting a profound modification in the reactivity landscape. One of the puzzling elements of VSC is the fact that these thermodynamic changes are typically an order of magnitude larger than the energy perturbation ($\leq k_B T$) associated with the Rabi splitting of the coupled vibration. This suggests that VSC must be inducing a fundamental change that leads to the observed modification in chemical reactivity. The most likely candidate is symmetry, which lies at the heart of chemical reactivity, as illustrated, for instance, by correlation diagrams between reactants and products.[15,16]

To explore the role of symmetry in VSC, we chose to study the charge transfer complexation of a highly symmetrical small molecule, the trimethylated benzene (mesitylene, or donor D) with iodine (acceptor A):

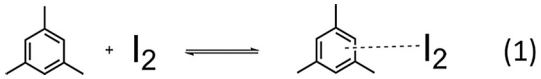

(1)

where K_{DA} is the equilibrium constant of the reaction. This CT complex is representative of the complexation of I_2 with aromatic molecules, first studied by Benesi and Hildebrand,[17] which gave rise to numerous experimental and theoretical studies, most notably by Mulliken.[18,19] Mulliken was able to explain many of the properties of such CT complexes by assuming a ground-state wavefunction of the type[19]

$$\Psi_i\,(\mathrm{DA}) = a\varphi_0\,(\mathrm{D,A}) + b\varphi_1(\mathrm{D^+A^-}), \tag{2}$$

in other words, a mixture of two states, $\varphi_0\,(\mathrm{D,A})$, the non-bonding but interacting pair of D and A, and $\varphi_1(\mathrm{D^+A^-})$, the ionic pair forming a weak covalent bond. The excited state is described in the same terms:

$$\Psi_f\,(\mathrm{DA}) = c\varphi_0\,(\mathrm{D,A}) + d\varphi_1(\mathrm{D^+A^-}) \tag{3}$$

It follows from this model that the transition energy between the ground- and excited states is $E_{if} = I_D + E_A + \Delta$, where I_D is the ionization potential of D, E_A the electron affinity of A, and Δ a correction term that includes various effects such as changes in the equilibrium position in the Morse potential, London dispersion forces, and the exchange integral. This charge-transfer transition gives rise to intense

[*] Y. Pang, A. Thomas, K. Nagarajan, R. M. A. Vergauwe, K. Joseph, B. Patrahau, K. Wang, C. Genet, T. W. Ebbesen
University of Strasbourg, CNRS, ISIS & icFRC
8 allée G. Monge, 67000 Strasbourg (France)
E-mail: genet@unistra.fr
ebbesen@unistra.fr

Supporting information and the ORCID identification number(s) for the author(s) of this article can be found under: https://doi.org/10.1002/anie.202002527.

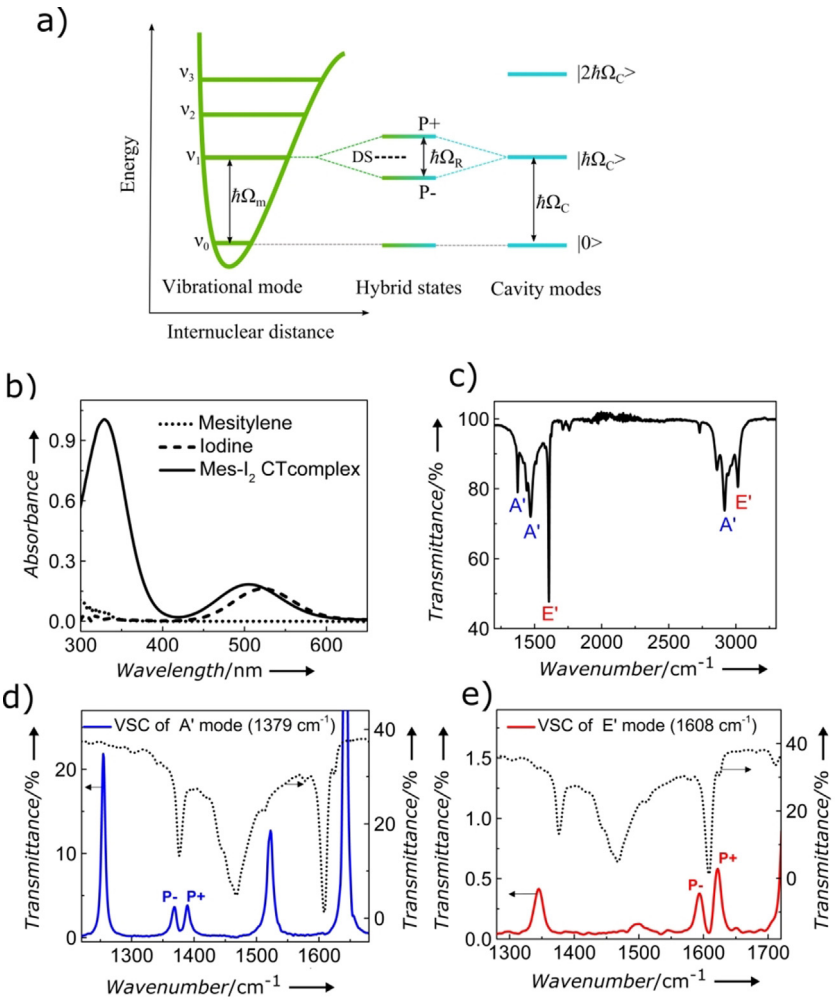

Figure 1. a) Schematic illustration of the strong coupling between a vibrational transition and a resonant Fabry–Perot (FP) cavity mode, leading to the formation of the hybrid vibropolaritonic states P+ and P− separated by the Rabi-splitting energy $\hbar\Omega_R$ and dark states (DS). b) Absorption spectra of mesitylene, iodide, and their charge-transfer complex. c) IR spectrum of mesitylene with the symmetry of the different vibrational modes. d), e) Example of a FP mode (blue line) splitting into P+ and P− by strongly coupling to an *A′* (d) and *E′* (e) vibrational mode.

bands in the UV spectrum (see, for example, Figure 1b). Such peaks can be used to monitor their equilibrium [Eq. (1)] and determine K_{DA} as well as the absorption coefficient ε_{DA} of the complex as explained further down.[20] For the purpose of this study, we note that the IR spectrum of mesitylene has a number of vibrational transitions which correspond to normal modes which belong either to the symmetry class *E′* or *A′* (see Figure 1c and the Supporting Information).[21] These vibrations can be strongly coupled by placing a solution of the sample in a microfluidic Fabry–Perot (FP) cavity and tuning the spacing between the mirrors so that one of the cavity modes is in resonance at normal incidence with the vibration to be coupled (Figure 1d,e). Under strong-coupling conditions, the original peak splits into two new peaks, which appear in the IR spectrum, reflecting the transitions to P+ and P−. The split peak is not in itself a proof of strong coupling, additionally, the separation of the peaks must be larger than the FWHM (full width at half maximum) of the IR-absorption peak and the cavity mode to achieve strong coupling, as will be illustrated in the next paragraphs. For further explanations about strongly coupled molecules, please see ref. [14].

The microfluidic FP cavity was constructed with CaF_2 windows coated with 10 nm Au and protected with 200 nm of spin-coated polyvinyl alcohol. The two mirrors were separated by a 25 μm Mylar spacer. Following an approach described in the literature,[20] I_2 was added to a solution of mesitylene in heptane (see the Supporting Information) and injected into the FP cavity. The tuning of the cavity and the Rabi splitting was then monitored with a FTIR spectrometer and the absorption spectrum of the CT complex inside the cavity was then recorded in the UV/Vis region for each value of the initial mesitylene concentration $[Mes]_0$. K_{DA} and ε_{DA} were then obtained by tracing the data according to Eq. (4) to obtain the so-called

$$\frac{[I_2]_0}{abs} = \frac{1}{\varepsilon_{DA} l} + \frac{1}{K_{DA}\varepsilon_{DA} l}\left(\frac{1}{[Mes]_0}\right), \qquad (4)$$

Benesi–Hildebrand plot

where abs is the absorbance of the CT peak at 330 nm, l is the path length of the cavity and, $[I_2]_0$ is the initial iodine concentration.

Figure 2a shows the evolution of the plot according to Eq. (4) upon varying $[Mes]_0$ values inside a cavity tuned to the 3017 cm^{-1} mode. As can be seen, two regimes can be distinguished with an abrupt discontinuity in between, akin to a phase transition. It was recorded over a small range to illustrate the sharpness of the transition. At low concentrations, the system behaves very much like it does in a normal cuvette, then suddenly upon reaching the strong-coupling condition, that is, the Rabi splitting is larger than the FWHM of the cavity mode and the vibrational band, a new slope is observed giving different values for K_{DA} and ε_{DA}. Before discussing this observation in more detail, we analyze the effects of VSC of the different vibrational modes of Mes on the CT equilibrium.

Figure 2b–d shows the UV/Vis-spectral changes associated with equilibrium Eq. (1) and the resulting plots according to Eq. (4) for three different situations. For the non-cavity, $K_{DA} = 0.40$ (Figure 2b), while it decreases fourfold to 0.09 for VSC of the 2915 cm^{-1} transition (Figure 2c). In contrast, the complexation constant more than doubles to 1.01 for VSC of the 1608 cm^{-1} mode (Figure 2d). Because the spectra are collected in the microfluidic cells with a very small path length (25 um), the changes in absorbances are also small and, additionally, they have to be corrected for background transmission. As a consequence, the spectra are noisy, and the Benesi–Hildebrand plots were averaged over a minimum

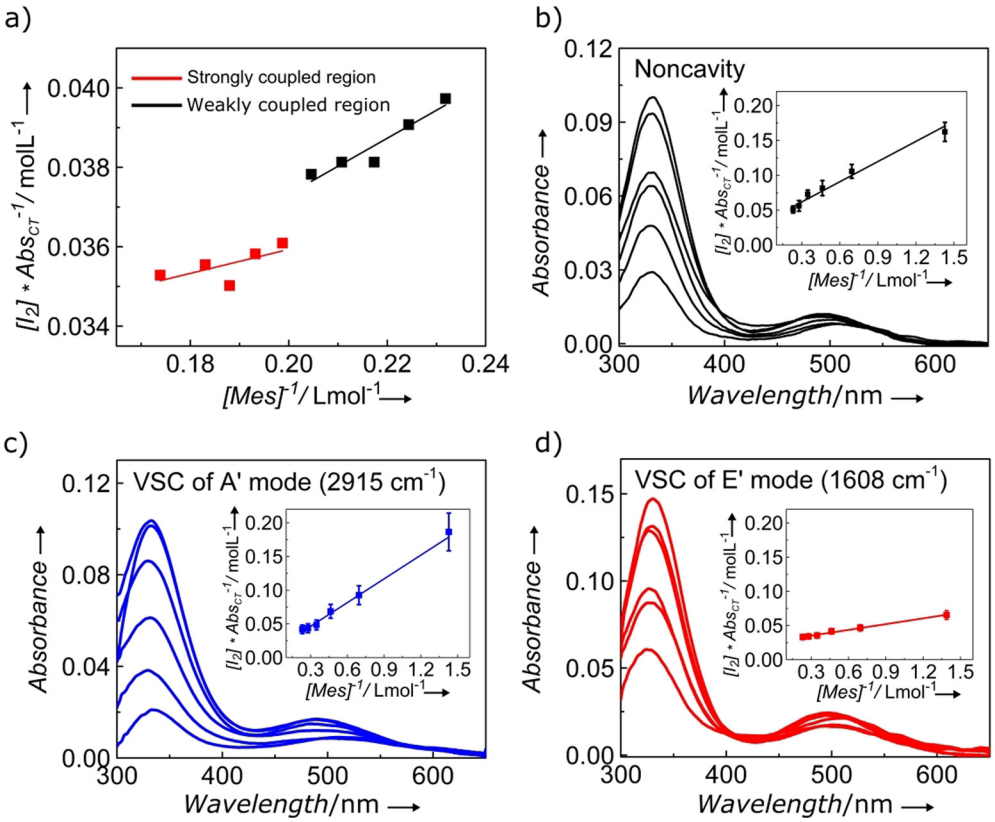

Figure 2. a) Benesi–Hildebrand plot revealing the transition from weakly to strongly coupled regimes when the cavity is resonant with the E' 3017 cm^{-1} vibration. b) Change in the absorption spectrum of the CT complex as a function of mesitylene concentration with (in the inset) the corresponding Benesi–Hildebrand plot for the out-of-resonance condition. c) The same for an A' vibration at 2915 cm^{-1} strongly coupled to a resonant cavity mode. d) The same for an E' vibration at 1608 cm^{-1} strongly coupled to a resonant cavity mode. Error bars show standard deviations of three or more experiments.

of three experiments and analyzed at the 330 nm peak. The observed changes in the equilibrium constants are much larger than the ±10% error in the experiments, as can be seen for the reference values in Table 1.

By further coupling other normal vibrations, it becomes clear that coupling A' modes lead to large decreases in K_{DA} while E' modes under VSC lead to increases, as summarized in Table 1. Additionally, it can be seen that the magnitude of change for both symmetries is mostly independent of the frequency of the coupled mode and the type of vibration. We also note that the Benesi–Hildebrand plots are linear over the range of $[Mes]_0$ concentrations used in these experiments. This is remarkable considering the fact that the Rabi splitting is proportional to the square root of $[Mes]_0$,[14] indicating again that the VSC-modified values of K_{DA} are only determined over the range of the study by the symmetry once the strong-coupling regime is reached. In other words, at the onset of strong coupling, the symmetry factors responsible for changes to K_{DA} are established and the complexation equilibrium was not impacted further with the increase in the Rabi-splitting energy in the studied range. These findings are further confirmed by the fact that deuterated mesitylene gives very similar results for both uncoupled and coupled conditions (Table 1 and Figure S2D in the Supporting Information) despite the large isotope-induced shift in the vibrational frequencies. Furthermore, the absence of vibrational modes in the 2500–3200 cm^{-1} region of deuterated mesitylene (Figure S2A) allowed us to study the impact of the VSC of the C–H stretching mode of heptane (solvent) on the CT equilibrium. Coupling the solvent vibrations alone did not shift the complexation equilibrium (off-resonance (d_{12}) in Table 1 and Figure S2D, black line) in the present experiments. We have also checked the case of benzene–I_2 complexation under VSC which only has E modes in the accessible wavelength range (Figure S4). It displays the same trend as the E' modes of the Mes–I_2 system (see Table 1 and the Supporting Information).

Another interesting feature of the results summarized in Table 1 lies in the variations in the CT-absorption cross-section ε_{DA} at 330 nm induced by VSC. Again, symmetry is playing a role, since changes are very large only when coupling the A' vibrations, with ε_{DA} increasing by as much as a factor of 3. A possible explanation can be probably be found in the various conformations that the CT complex can take. The conformations of such complexes have been extensively studied and discussed.[18,22] For instance, of all the possible conformers for the benzene–I_2 complex, it has been established that the most likely ones are the "oblique" with the I_2 axis at an oblique angle above the benzene ring, the "above carbon" and the "above bond" where the I_2 is oriented perpendicular to the aromatic plane above a C atom or a C–C bond, respectively. These are also favored on symmetry considerations.[18] Furthermore, a detailed theoretical study[22] shows that only those three conformers have significant oscillator strengths and, therefore, will contribute to the CT band. At the same time, there are large differences between them. In solution at room temperature, it is reasonable to assume that the Mes–I_2 complex fluctuates between such conformations, since the $\Delta G°$ of complexation is on the order or less than $k_B T$ (Table 2). With this in mind, the increase in ε_{DA} observed for the Mes–I_2 complex under VSC could be explained by the fact the coupling favors a high-oscillator-strength conformer over the others. Interestingly, according to quantum-chemical calculations on the benzene–I_2 complex, the oscillator

Table 1: CT-complexation equilibrium constants and absorption coefficient of the complex. Frequencies given in cm^{-1}, ε_{DA}(330 nm) values given in $10^4\ mol^{-1}\,L\,cm^{-1}$.

experiment	vibrational mode	K	ε_{DA}(330 nm)
mesitylene–iodine			
non-cavity[a]		0.40 ± 0.04	1.38 ± 0.2
non-cavity[b]		0.41 ± 0.02	1.44 ± 0.1
off-resonance		0.47 ± 0.05	1.68 ± 0.2
off-resonance (d_{12})[c]		0.40 ± 0.04	1.56 ± 0.2
on-resonance	2915 (A')	0.09 ± 0.01	3.82 ± 0.4
	1468 (A')	0.16 ± 0.02	3.63 ± 0.4
	1379 (A')	0.15 ± 0.02	4.70 ± 0.5
	3017 (E')	1.03 ± 0.1	1.36 ± 0.2
	1608 (E')	1.01 ± 0.1	1.52 ± 0.2
	1580 (d_{12}, E')[d]	1.20 ± 0.1	1.23 ± 0.12
benzene–iodine			
non-cavity[a]		0.15 ± 0.02	0.65 ± 0.05
off-resonance		0.15 ± 0.02	0.65 ± 0.06
on-resonance	3040 (E_{1u})	0.62 ± 0.06	0.53 ± 0.05
	1480 (E_{1u})	0.65 ± 0.06	0.45 ± 0.05

[a] Non-cavity experiment carried out in a 25 μm path-length cell, [b] non-cavity experiment carried out with a 1 mm path-length quartz cuvette, [c] experiment with mesitylene-d_{12}, where the cavity mode was on resonance only with the C–H stretching vibrational mode of heptane at 2915 cm^{-1}, and [d] on-resonance with the E' vibrational mode of mesitylene-d_{12}.

Table 2: Thermodynamics of complexation (298 K). All values given in $kJ\,mol^{-1}$.

experiment	$\Delta H°$	$T\Delta S°$	$\Delta G°$
non-cavity	−19.6	−21.8	2.2
VSC, E' mode (1608 cm^{-1})	−13.4	−13.5	0.1
VSC, A' mode (2915 cm^{-1})	−39.7	−45.6	5.9

strength of the CT complex increases as the axial I_2 position shifts towards the C–C bond of the benzene ring.[22] This suggest that the increase in ε_{DA} for the A' mode of mesitylene under VSC corresponds to a lowering of the axial symmetry of the Mes–I_2 complex, and thereby destabilizes the complex, as observed by K_{DA}.

We have analyzed the temperature dependence of the reaction to extract the $\Delta H°$ and $\Delta S°$ values of the complexation outside the cavity and under VSC for the two symmetries (Figure S3). The results, summarized in Table 2, show that $\Delta H°$ and $\Delta S°$ change significantly, way beyond the Rabi splittings which are all less than $k_B T$ ($<2.5\ kJ\,mol^{-1}$). While earlier thermodynamic values reported for reactions under VSC only considered the change in the barrier, that is, the activation energy, these changes reflect the relative modification $\Delta G°$ of the ground-state energy of the reactants and the products. In other words, it is surprising to see that the ground-state energy can be modified and tilted in both directions simply by splitting the vibrational transition through VSC as illustrated in Figure 3.

As can be seen in Figure 2a, the onset of strong coupling totally changes the properties of the system as it switches from one set of eigenstates to a new one incorporating the polaritonic states. Thermodynamic data confirms the other findings of this study, namely that the energetic perturbation induced by the Rabi splitting in the ladder of eigenstates cannot account for the changes observed. By selectively coupling vibrational modes, the central role of symmetry in the complexation under VSC is revealed by this study. It is well known that the correlation of symmetry between reactants and products influence the rate and outcome of chemical reactions.[15,16] Additionally, as analyzed by Bader,[16] the symmetry of vibrations plays a key role in favoring a reaction pathway over another through the interaction between vibrational and electronic manifolds. VSC must be modifying the symmetries of the correlation diagram of the CT complexation via such vibronic interactions. In this particular case studied here, both reactants and the complex are of A symmetry, as pointed out by Mulliken.[18] According to Bader,[16] a vibration of the same A symmetry in the reaction landscape will favor the complex. Since E'-symmetry vibrations under VSC favor complexation while A' vibrations do not, our results point to the fact that the onset of strong coupling leads to a change in the symmetry-correlation diagram. In the end, this is perhaps not so surprising since the molecular transition is hybridized with the electromagnetic field of the cavity to give a polaritonic wavefunction with a node (P–) at the lowest energy level, modifying the orbital interactions and the correlation diagram.

While the influence of polaritonic states on material and chemical properties is now well established, so far, the central focus of the analysis was on the energetics as it was not possible to see the role of symmetry in view of the complexity of the systems studied.[8–14,23–41] With this simple and highly symmetrical CT-complexation reaction, the key role of symmetry in strong coupling has now become very apparent.

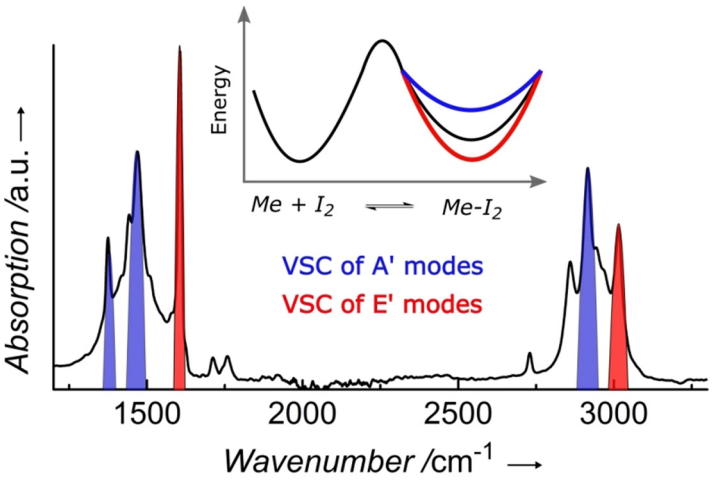

Figure 3. IR absorption spectrum of the mesitylene coupled vibrations with their symmetries E' (red) and A' (blue), together with the consequences on the CT equilbrium landscape of the mesitylene–I_2 complexation process in the inset. The latter shows the shift in the Gibbs free energy of the products vs. the reactants due to vibrational symmetry under VSC with the same colour code. While the activation barrier might also be changed, it was too small to affect equilibrium and could not be observed in these experiments.

As shown here, VSC can either favor or destabilize the equilibrium complexation depending on the symmetry of the coupled vibration, suggesting that such perturbations of the symmetry-correlation diagram between reactants and products might be at the origin of the acceleration and inhibition of the reactions studied to date under VSC.[8–13] By the capacity to selectively couple specific vibrations, VSC is a unique tool to analyze the influence of vibrations and symmetry classes on chemical reactivity. It also suggests that symmetry could be another parameter in strongly coupled materials and solid-state systems.

Acknowledgements

We acknowledge support of the International Center for Frontier Research in Chemistry (icFRC, Strasbourg), the ANR "ERA-NET QuantERA" – Projet "RouTe" (ANR-18-QUAN-0005-01), the ANR Equipex Union (ANR-10-EQPX-52-01), CSC (ANR-10-LABX- 0026 CSC) within the Investissement d'Avenir program ANR-10-IDEX-0002-02. T.W.E. acknowledges the support of the ERC (project no 788482 MOLUSC). Y.P. thanks the support of the China Scholarship Council (201808370031).

Conflict of interest

The authors declare no conflict of interest.

Keywords: charge transfer · light–matter strong coupling · polaritonic chemistry · symmetry · vibrations

[1] H. Frei, L. Fredin, G. C. Pimentel, *J. Chem. Phys.* **1981**, *74*, 397 – 411.
[2] Q. Wang, R. W. Schoenlein, L. A. Peteanu, R. A. Mathies, C. V. Shank, *Science* **1994**, *266*, 422 – 424.
[3] R. N. Zare, *Science* **1998**, *279*, 1875 – 1879.
[4] W. Zhang, H. Kawamata, K. Liu, *Science* **2009**, *325*, 303 – 306.
[5] M. Delor, I. V. Sazanovich, M. Towrie, J. A. Weinstein, *Acc. Chem. Res.* **2015**, *48*, 1131 – 1139.
[6] Z. Lin, C. M. Lawrence, D. Xiao, V. V. Kireev, S. S. Skourtis, J. L. Sessler, D. N. Beratan, I. V. Rubtsov, *J. Am. Chem. Soc.* **2009**, *131*, 18060 – 18062.
[7] A. A. Bakulin, R. Lovrincic, X. Yu, O. Selig, H. J. Bakker, Y. L. A. Rezus, P. K. Nayak, A. Fonari, V. Coropceanu, J.-L. Brédas, et al., *Nat. Commun.* **2015**, *6*, 7880.
[8] A. Thomas, J. George, A. Shalabney, M. Dryzhakov, S. J. Varma, J. Moran, T. Chervy, X. Zhong, E. Devaux, C. Genet, et al., *Angew. Chem. Int. Ed.* **2016**, *55*, 11462 – 11466; *Angew. Chem.* **2016**, *128*, 11634 – 11638.
[9] H. Hiura, A. Shalabney, J. George, *ChemRxiv* **2018**, https://doi.org/10.26434/chemrxiv.7234721.v2.
[10] J. Lather, P. Bhatt, A. Thomas, T. W. Ebbesen, J. George, *Angew. Chem. Int. Ed.* **2019**, *58*, 10635 – 10638; *Angew. Chem.* **2019**, *131*, 10745 – 10748.
[11] A. Thomas, L. LethuillierKarl, K. Nagarajan, R. M. A. Vergauwe, J. George, T. Chervy, A. Shalabney, E. Devaux, C. Genet, J. Moran, et al., *Science* **2019**, *363*, 615 – 619.
[12] R. M. A. Vergauwe, A. Thomas, K. Nagarajan, A. Shalabney, J. George, T. Chervy, M. Seidel, E. Devaux, V. Torbeev, T. W. Ebbesen, *Angew. Chem. Int. Ed.* **2019**, *58*, 15324 – 15328; *Angew. Chem.* **2019**, *131*, 15468 – 15472.
[13] K. Hirai, R. Takeda, J. Hutchison, H. Uji-I, *Angew. Chem. Int. Ed.* **2020**, *59*, 5332 – 5335; *Angew. Chem.* **2020**, *132*, 5370 – 5373.
[14] T. W. Ebbesen, *Acc. Chem. Res.* **2016**, *49*, 2403 – 2412.
[15] R. B. Woodward, R. Hoffmann, *Angew. Chem. Int. Ed. Engl.* **1969**, *8*, 781 – 932; *Angew. Chem.* **1969**, *81*, 797 – 869.
[16] R. Bader, *Can. J. Chem.* **1962**, *40*, 1164 – 1175.
[17] H. A. Benesi, J. H. Hildebrand, *J. Am. Chem. Soc.* **1949**, *71*, 2703 – 2707.
[18] R. S. Mulliken, *J. Am. Chem. Soc.* **1952**, *74*, 811 – 824.
[19] C. J. Bender, *Chem. Soc. Rev.* **1986**, *15*, 475 – 502.
[20] J. C. Baum, C. J. Marzzacco, C. Kendrow, *J. Chem. Educ.* **2009**, *86*, 1330 – 1334.
[21] B. V. Lokshin, V. T. Aleksanyan, M. G. Ezernitskaya, *Russ. Chem. Bull.* **1982**, *31*, 1995 – 1999.
[22] F. C. Grozema, R. W. J. Zijlstra, M. Swart, P. T. Van Duijnen, *Int. J. Quantum Chem.* **1999**, *75*, 709 – 723.
[23] C. Schäfer, M. Ruggenthaler, H. Appel, A. Rubio, *Proc. Natl. Acad. Sci. USA* **2019**, *116*, 4883 – 4892.
[24] J. Flick, C. Schäfer, M. Ruggenthaler, H. Appel, A. Rubio, *ACS Photonics* **2018**, *5*, 992 – 1005.
[25] J. Galego, F. J. Garcia-Vidal, J. Feist, *Nat. Commun.* **2016**, *7*, 13841.
[26] J. Galego, F. J. Garcia-Vidal, J. Feist, *Phys. Rev. Lett.* **2017**, *119*, 136001.
[27] F. Herrera, F. C. Spano, *Phys. Rev. Lett.* **2016**, *116*, 238301.
[28] J. A. Campos-Gonzalez-Angulo, R. F. Ribeiro, J. Yuen-Zhou, *Nat. Commun.* **2019**, *10*, 1 – 8.
[29] J. A. Hutchison, T. Schwartz, C. Genet, E. Devaux, T. W. Ebbesen, *Angew. Chem. Int. Ed.* **2012**, *51*, 1592 – 1596; *Angew. Chem.* **2012**, *124*, 1624 – 1628.
[30] E. Orgiu, J. George, J. A. Hutchison, E. Devaux, J. F. Dayen, B. Doudin, F. Stellacci, C. Genet, J. Schachenmayer, C. Genes, et al., *Nat. Mater.* **2015**, *14*, 1123 – 1129.
[31] X. Zhong, T. Chervy, L. Zhang, A. Thomas, J. George, C. Genet, J. A. Hutchison, T. W. Ebbesen, *Angew. Chem. Int. Ed.* **2017**, *56*, 9034 – 9038; *Angew. Chem.* **2017**, *129*, 9162 – 9166.
[32] G. Groenhof, J. J. Toppari, *J. Phys. Chem. Lett.* **2018**, *9*, 4848 – 4851.
[33] K. Stranius, M. Hertzog, K. Börjesson, *Nat. Commun.* **2018**, *9*, 2273.
[34] S. Wang, T. Chervy, J. George, J. M. Hutchison, C. Genet, T. W. Ebbesen, *J. Phys. Chem. Lett.* **2014**, *5*, 1433 – 1439.
[35] R. Damari, O. Weinberg, D. Krotkov, N. Demina, K. Akulov, A. Golombek, T. Schwartz, S. Fleischer, *Nat. Commun.* **2019**, *10*, 3248.
[36] W. Ahn, I. Vurgaftman, A. D. Dunkelberger, J. C. Owrutsky, B. S. Simpkins, *ACS Photonics* **2018**, *5*, 158 – 166.
[37] V. F. Crum, S. R. Casey, J. R. Sparks, *Phys. Chem. Chem. Phys.* **2018**, *20*, 850 – 857.
[38] L. Munkhbat, M. Wersäll, D. G. Baranov, T. J. Antosiewicz, T. Shigai, *Sci. Adv.* **2018**, *4*, eaas9552.
[39] D. Hagenmüller, J. Schachenmayer, S. Schütz, C. Genes, G. Pupillo, *Phys. Rev. Lett.* **2017**, *119*, 223601.
[40] G. L. Paravicini-Bagliani, F. Appugliese, E. Richter, F. Valmorra, J. Keller, M. Beck, N. Bartolo, C. Rössler, T. Ihn, K. Ensslin, et al., *Nat. Phys.* **2019**, *15*, 186 – 190.
[41] N. Bartolo, C. Ciuti, *Phys. Rev. B* **2018**, *98*, 205301.

Manuscript received: February 18, 2020
Accepted manuscript online: March 27, 2020
Version of record online: April 16, 2020

